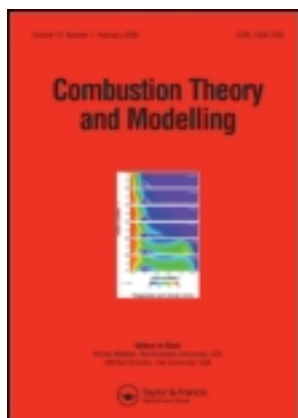


This article was downloaded by: [University of California, San Diego]
On: 05 July 2012, At: 12:22
Publisher: Taylor & Francis
Informa Ltd Registered in England and Wales Registered Number: 1072954 Registered office: Mortimer House, 37-41 Mortimer Street, London W1T 3JH, UK



Combustion Theory and Modelling

Publication details, including instructions for authors and subscription information:

<http://www.tandfonline.com/loi/tctm20>

Ignition and extinction of low molecular weight esters in nonpremixed flows

Ulrich Niemann^a, Reinhard Seiser^a & Kalyanasundaram Seshadri^a

^a Department of Mechanical and Aerospace Engineering,
University of California at San Diego, La Jolla, California,
92093-0411

Version of record first published: 21 Oct 2010

To cite this article: Ulrich Niemann, Reinhard Seiser & Kalyanasundaram Seshadri (2010): Ignition and extinction of low molecular weight esters in nonpremixed flows, *Combustion Theory and Modelling*, 14:6, 875-891

To link to this article: <http://dx.doi.org/10.1080/13647830.2010.517275>

PLEASE SCROLL DOWN FOR ARTICLE

Full terms and conditions of use: <http://www.tandfonline.com/page/terms-and-conditions>

This article may be used for research, teaching, and private study purposes. Any substantial or systematic reproduction, redistribution, reselling, loan, sub-licensing, systematic supply, or distribution in any form to anyone is expressly forbidden.

The publisher does not give any warranty express or implied or make any representation that the contents will be complete or accurate or up to date. The accuracy of any instructions, formulae, and drug doses should be independently verified with primary sources. The publisher shall not be liable for any loss, actions, claims, proceedings, demand, or costs or damages whatsoever or howsoever caused arising directly or indirectly in connection with or arising out of the use of this material.

Ignition and extinction of low molecular weight esters in nonpremixed flows

Ulrich Niemann, Reinhard Seiser and Kalyanasundaram Seshadri*

*Department of Mechanical and Aerospace Engineering, University of California at San Diego,
La Jolla, California 92093-0411*

(Received 8 April 2010; final version received 11 August 2010)

An experimental and kinetic modeling study is carried out to characterize combustion of low molecular weight esters in nonpremixed, nonuniform flows. An improved understanding of the combustion characteristics of low molecular weight esters will provide insights on combustion of high molecular weight esters and biodiesel. The fuels tested are methyl butanoate, methyl crotonate, ethyl propionate, biodiesel, and diesel. Two types of configuration – the condensed fuel configuration and the prevaporized fuel configuration – are employed. The condensed fuel configuration is particularly useful for studies on those liquid fuels that have high boiling points, for example biodiesel and diesel, where prevaporization, without thermal breakdown of the fuel, is difficult to achieve. In the condensed fuel configuration, an oxidizer, made up of a mixture of oxygen and nitrogen, flows over the vaporizing surface of a pool of liquid fuel. A stagnation-point boundary layer flow is established over the surface of the liquid pool. The flame is stabilized in the boundary layer. In the prevaporized fuel configuration, the flame is established in the mixing layer formed between two streams. One stream is a mixture of oxygen and nitrogen and the other is a mixture of prevaporized fuel and nitrogen. Critical conditions of extinction and ignition are measured. The results show that the critical conditions of extinction of diesel and biodiesel are nearly the same. Experimental data show that in general flames burning the esters are more difficult to extinguish in comparison to those for biodiesel. At the same value of a characteristic flow time, the ignition temperature for biodiesel is lower than that for diesel. The ignition temperatures for biodiesel are lower than those for the methyl esters tested here. Critical conditions of extinction and ignition for methyl butanoate were calculated using a detailed chemical kinetic mechanism. The results agreed well with the experimental data. The asymptotic structure of a methyl butanoate flame is found to be similar to that for many hydrocarbon flames. This will facilitate analytical modeling, of structures of ester flames, using rate-ratio asymptotic techniques, developed previously for hydrocarbon flames.

Keywords: esters; nonpremixed flames; extinction; ignition; biodiesel

1. Introduction

There is considerable interest in understanding the combustion of esters because they are considered as possible surrogates of biodiesel [1–12]. The components in biodiesel are generally methyl, ethyl, or higher alkyl esters. Numerous experimental and modeling studies have been carried out on combustion of methyl butanoate ($n\text{-C}_3\text{H}_7\text{C}(=\text{O})\text{OCH}_3$) [3–8]

*Corresponding author. Email: seshadri@ucsd.edu

and methyl decanoate ($n\text{-C}_9\text{H}_{19}\text{C}(=\text{O})\text{OCH}_3$) [10–12], because kinetic models describing the combustion of these fuels are expected to be used as “building blocks” for describing combustion of biodiesel. Methyl decanoate is a high molecular weight ester. Kinetic models describing combustion of methyl butanoate [3–7] and methyl decanoate [10–12] have been developed and tested by comparison with experimental data obtained in shock tubes, rapid compression machines, flow reactors, and counterflow nonpremixed flames. These previous studies on methyl butanoate did not measure or predict critical conditions of extinction and ignition in flow systems [3–8]. A previous experimental and kinetic modeling study was carried out on the combustion of methyl decanoate in nonpremixed, nonuniform flows [11]. Experiments were performed employing the counterflow configuration. Critical conditions of extinction and ignition were measured. Kinetic modeling was performed using a skeletal chemical-kinetic mechanism that was derived from a detailed mechanism. Critical conditions of extinction and ignition were calculated using this skeletal mechanism and they were found to agree well with experimental data [11]. In this previous study, the critical conditions of extinction or ignition of methyl decanoate were not directly compared with those of biodiesel. Here, the previously measured experimental data on methyl decanoate are compared with those for other esters and also with that of biodiesel.

The present experimental and kinetic modeling study is focused on characterizing key aspects of combustion of low molecular weight esters in nonpremixed nonuniform flows. Combustion processes in diesel engines closely resemble nonpremixed systems, and ignition plays a key role. Critical conditions of ignition and extinction are measured for nonpremixed combustion of methyl butanoate, methyl crotonate ($\text{CH}_3\text{C}=\text{CH}(\text{C}=\text{O})\text{OCH}_3$), ethyl propionate ($\text{C}_2\text{H}_5\text{C}(=\text{O})\text{OC}_2\text{H}_5$), n -heptane ($n\text{-C}_7\text{H}_{16}$), biodiesel (made from soybeans), and diesel. The volumetric composition of biodiesel employed in this study was (reported by the manufacturer) methyl palmitate (11%), methyl stearate (4%), methyl oleate (17%), methyl linoleate (67%), and methyl linolenate (1%). The diesel was obtained from a local station. Experimental data is also obtained for a mixture of 20% methyl butanoate and 80% n -heptane by volume, because n -heptane was previously considered as a surrogate for diesel and studies on combustion of this mixture is expected to elucidate key aspects of combustion of mixtures of biodiesel and diesel. The knowledge obtained from studies on low molecular weight esters is expected to be building blocks for future studies on high molecular weight methyl esters. In addition, the present study provides fundamental knowledge on some key aspects of combustion of esters.

2. Experimental apparatus, procedures, and results

To capture the influence of the flow field on the critical conditions of ignition and flame extinction, experiments are conducted in the counterflow configuration. Two types of configurations – the condensed fuel configuration and the prevaporized fuel configuration – are employed. The condensed fuel configuration is particularly useful for studies on those liquid fuels that have high boiling points, for example biodiesel and diesel, where prevaporization, with negligible thermal breakdown, is difficult to achieve. In general, many liquid fuels can be tested in the condensed fuel configuration, while only those fuels with boiling points less than 600 K can be safely tested in the prevaporized fuel configuration. At higher temperatures, cracking of the fuel can take place. In the prevaporized fuel configuration, the mass fraction and mass flux of fuel in the fuel stream are independent variables under the control of the experimenter, while these quantities are dependent variables in the condensed

Table 1. Properties of some esters, biodiesel, and diesel.

Name	Chemical symbol	Normal boiling point [K]	Molecular weight [kg/mol]
Methyl crotonate	$C_5H_8O_2$	392	0.1
Methyl butanoate	$C_5H_{10}O_2$	375	0.102
Ethyl propionate	$C_5H_{10}O_2$	372	0.102
Methyl decanoate	$C_{11}H_{22}O_2$	497	0.186
<i>n</i> -Heptane	C_7H_{16}	372	0.1
Biodiesel	C:H:O= 19:36:2	626–716	0.294
Diesel	C:H = 16:26	448–623	0.218

fuel configuration and cannot be independently controlled by the experimenter. Thus the prevaporized fuel configuration allows experiments to be conducted over a wider range of parameters. Table 1 shows some relevant properties of the fuels tested here. It shows that the boiling point of biodiesel is between 626 K and 716 K. Therefore, this fuel is tested in the condensed fuel configuration. The boiling point of all methyl esters tested here is less than 500 K. Therefore, these fuels can be tested in both configurations. In this work, biodiesel, diesel, and methyl butanoate are tested in the condensed fuel configuration. The other esters including methyl butanoate are tested in the prevaporized configuration. By comparing the combustion characteristics of methyl butanoate with biodiesel, and methyl butanoate with other esters, it was possible to compare the combustion characteristics of all esters tested here with biodiesel.

2.1. Condensed fuel configuration

A detailed description of the counterflow burner used for carrying out experiments in the condensed fuel configuration is given elsewhere [13]. This burner has been successfully employed previously to carry out experiments on a wide variety of liquid fuels, including high boiling point fuels, jet fuels, and other multicomponent liquid fuels [13–15].

Figure 1 shows a schematic illustration of the condensed fuel configuration. An axisymmetric stagnation-point flow of a gaseous oxidizer stream over the surface of an evaporating pool of a liquid fuel is considered. The oxidizer stream is a mixture of oxygen (O_2) and nitrogen (N_2). It is injected from the oxidizer-duct. The exit of the oxidizer-duct is the oxidizer boundary. Fine mesh wire screens are placed at the exit of the oxidizer-duct. As

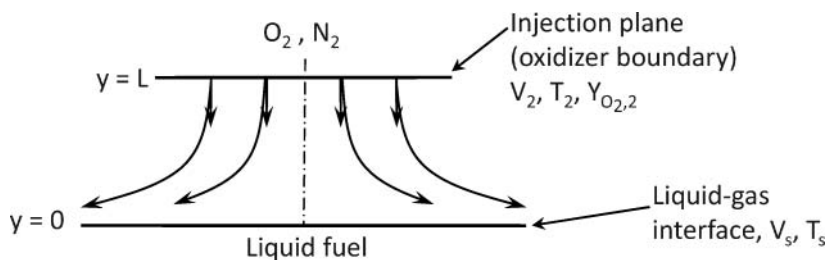


Figure 1. Schematic illustration of the condensed fuel configuration. V_2 and V_s are the velocities at the oxidizer-injection and the gas side of the liquid–gas interface planes, respectively. T_2 and T_s are the temperatures at the oxidizer-injection and the liquid–gas interface planes, respectively.

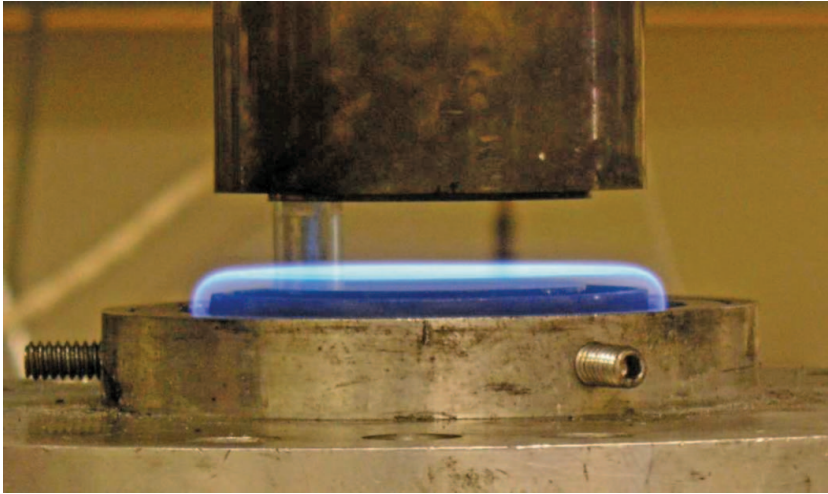


Figure 2. Photograph of a methyl butanoate flame stabilized the condensed fuel configuration.

a consequence, the radial component of the flow velocity is zero at the oxidizer boundary. This allows the use of no-slip boundary conditions (plug flow boundary conditions). The origin is placed on the axis of symmetry at the surface of the liquid pool. The distance between the surface of the liquid pool and the oxidizer boundary is L . At the oxidizer boundary, the injection velocity is V_2 , the temperature T_2 , the density ρ_2 , and the mass fraction of oxygen $Y_{O_2,2}$. Here, subscript 2 represents conditions at the oxidizer boundary. The magnitude of the injection velocity, V_2 , is estimated from the ratio of the measured volumetric flowrate of the oxidizer stream and the cross-section area of the oxidizer-duct. The temperature at the liquid–gas interface is T_s , and the mass averaged velocity on the gas side of the liquid–gas interface is V_s . Here, subscript s represents conditions on the gas side of the liquid–gas interface. It has been shown by use of asymptotic analysis [13] that the radial velocity on the gas side of the liquid–gas interface is small and can be set equal to zero. Asymptotic analysis of the flow field in the limit of large values of the Reynolds number at the oxidizer boundary was carried out previously [16]. The analysis shows that a thin boundary layer is established at the surface of the liquid pool. The inviscid flow outside the boundary layer is rotational. The local strain rate, a_2 , at the stagnation plane is given by [13, 16].

$$a_2 = 2V_2/L. \quad (1)$$

Figure 2 shows a photograph of a methyl butanoate flame stabilized in the condensed fuel configuration.

The condensed fuel configuration shown in Figure 1 is an open system because the fuel evaporating from the liquid–gas interface is continuously replenished from a reservoir. In experiments with fuel mixtures, where the boiling point of various components in the mixture is not the same, the concentration of the various components in the mixture on the liquid side of the liquid–gas interface will be different from that in the reservoir. This would result in diffusion of various components of the fuel mixture in the liquid. After steady state has been achieved, the sum of the convective and diffusive flux of each component

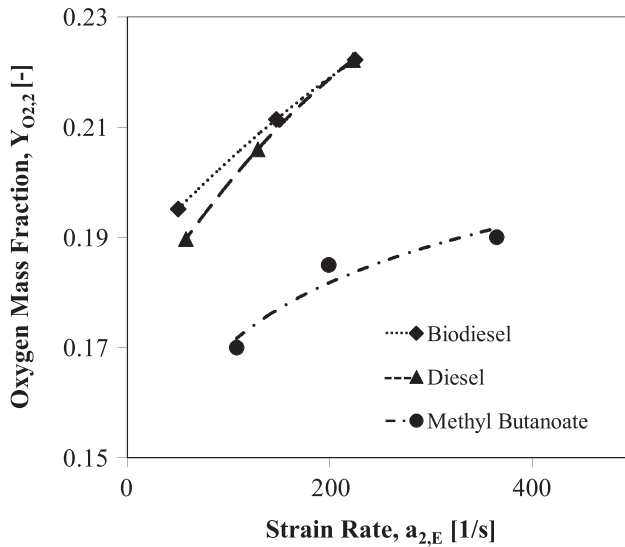


Figure 3. The mass fraction of oxygen in the oxidizer stream, $Y_{O_{2,2}}$, as a function of the strain rate at extinction, $a_{2,e}$. The symbols represent experimental data. The lines are best fit to the data. The experimental data was obtained in the condensed fuel configuration.

transported toward the liquid–gas interface will be proportional to its mass fraction in the reservoir. Therefore, on the gas side of the liquid–gas interface, the sum of the convective and diffusive flux of each component transported away from the interface will be also be proportional to its mass fraction in the reservoir. Accurate interpretation of experimental data obtained in the condensed fuel configuration is possible if the system attains steady state quickly. Previous studies on fuel mixtures have clearly demonstrated that extinction experiments can be performed employing the condensed fuel configuration because the system attains steady state quickly [15, 17, 18].

In the condensed fuel configuration, extinction experiments are performed with $T_2 = 298$ K, and $L = 10$ mm. At a given value of $Y_{O_{2,2}}$, the velocity V_2 is increased until extinction takes place. The strain rate at extinction is calculated using Equation (1). It is represented by $a_{2,e}$. The experiments are repeated at different values of $Y_{O_{2,2}}$. The accuracy of the strain rate is $\pm 10\%$ of recorded value and that of $Y_{O_{2,2}}$ is $\pm 3\%$ of recorded value. The measurement repeatability of strain rate is $\pm 2\%$ that of $Y_{O_{2,2}}$ is $\pm 2\%$, and temperature $\pm 1\%$.

Figure 3 shows $Y_{O_{2,2}}$ as a function of $a_{2,e}$ for biodiesel, diesel, and methyl butanoate. The symbols represent experimental data. The lines are best fit to the data. A line connecting the experimental data for any fuel represents a boundary. The region above the curve is flammable. Figure 3 shows that the critical conditions of extinction of biodiesel and diesel are nearly the same. At a given $Y_{O_{2,2}}$, the strain rate at extinction for methyl butanoate is higher than those for biodiesel and diesel. This indicates that under the conditions tested here, methyl butanoate is harder to extinguish than biodiesel and diesel.

In the ignition experiments, the oxidizer stream is air and $L = 12$ mm. Here, for a given value of the flow velocity of the oxidizer stream, V_2 , its temperature, T_2 , is increased until ignition takes place. The value of T_2 at ignition is represented by $T_{2,1}$. The value of the

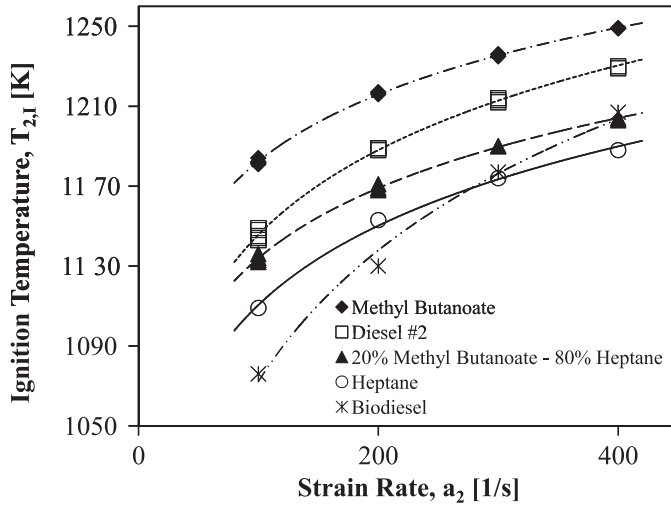


Figure 4. Experimental data showing the temperature of air at ignition, $T_{2,1}$, as a function of the strain rate. The symbols represent measurements. The lines are best fits to the experimental data. The experimental data was obtained employing the condensed fuel configuration.

strain rate is calculated using Equation (1). It is represented by $a_{2,1}$. The accuracy of the measurement of the temperature of air at ignition is expected to be ± 30 K, that of the strain rate ± 10 %. The experimental repeatability in the measurement of the temperature of air at ignition is expected to be ± 6 K. Values of $T_{2,1}$ are measured for various a_2 . Figure 4 shows measured critical conditions of ignition for methyl butanoate, *n*-heptane, a mixture of 20 % methyl butanoate and 80 % *n*-heptane by volume, diesel, and biodiesel. The symbols represent measurements. For a given fuel, a curve connecting the symbols is a boundary. Ignition does not take place in the region below this boundary. For all fuels tested, $T_{2,1}$ increases with increasing a_2 . For lower values of a_2 , the value of $T_{2,1}$ for methyl butanoate is the highest. Thus, at low values of a_2 , methyl butanoate is most difficult to ignite followed by diesel, the mixture, *n*-heptane, and biodiesel. At higher values of the strain rate, biodiesel is more difficult to ignite than *n*-heptane.

2.2. Prevaporized fuel configuration

A schematic illustration of the prevaporized fuel configuration is shown in Figure 5. A detailed description of the burner is given elsewhere [19]. Here, a fuel stream made up of prevaporized fuel and N_2 is injected from one duct, and an oxidizer stream made up of O_2 and N_2 is injected from the other duct. Fine wire mesh screens are placed at the exit of the fuel-duct and at the exit of the oxidizer-duct. This allows the use of no-slip boundary conditions at the fuel boundary and at the oxidizer boundary. The injection velocities of the fuel stream and the oxidizer stream at the fuel boundary and oxidizer boundary are represented by V_1 and V_2 , respectively. Their magnitudes are estimated from the ratio of the measured volumetric flow rates of the fuel stream and the oxidizer stream and the cross-section area of the ducts. The temperatures of the fuel stream and the oxidizer stream at the boundaries are T_1 and T_2 , respectively. The distance between the injection planes is L . The local strain rate on the oxidizer side of the stagnation plane, a_2 , is given by the

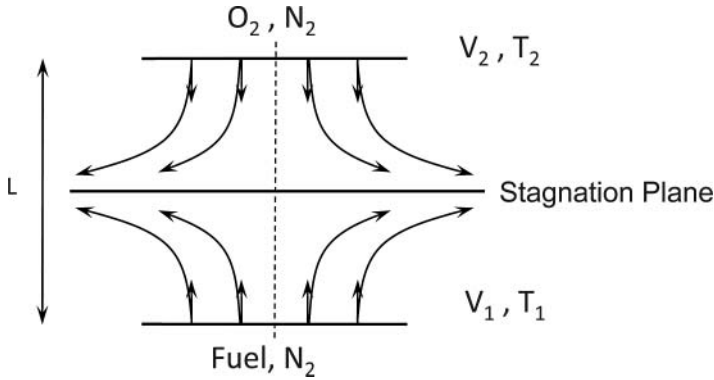


Figure 5. Schematic illustration of the prevaporized fuel configuration. V_2 and T_2 are the velocity and temperature at the oxidizer-injection plane and V_1 and T_1 are the velocity and temperature at the fuel-injection plane.

expression [16],

$$a_2 = \frac{2|V_2|}{L} \left(1 + \frac{|V_1|\sqrt{\rho_1}}{|V_2|\sqrt{\rho_2}} \right), \quad (2)$$

where ρ_1 is the the density of the fuel stream at the fuel boundary, and ρ_2 is the the density at the oxidizer stream at the oxidizer boundary.

Extinction experiments are conducted with $L = 10$ mm, and $T_2 = 298$ K. The temperature of the fuel stream, T_1 , for methyl butanoate, methyl crotonate, and ethyl propionate are $453 (\pm 10)$ K, $448 (\pm 10)$ K, and $445 (\pm 10)$ K, respectively. The momenta of the counterflowing streams are balanced. Thus $\rho_1 V_1^2 = \rho_2 V_2^2$. At some selected value of $Y_{F,1}$, the flame is stabilized. The strain rate is increased by increasing V_1 and V_2 until extinction is observed. The accuracy of the measurement of the fuel mass fraction is $\pm 3\%$ of recorded value.

Figure 6 compares the critical conditions of extinction for various esters. It shows the mass fraction of fuel in the fuel stream, $Y_{F,1}$, as a function of the strain rate. The experimental data for methyl decanoate was obtained from Ref. [11]. The critical conditions of extinction of methyl decanoate, methyl butanoate, and methyl crotonate are nearly the same. At a given value of $Y_{F,1}$ the value of a_2 at extinction for ethyl propionate is much larger than that for methyl decanoate. Therefore, ethyl propionate is much more difficult to extinguish when compared with the other esters. Comparison of the data in Figure 6 with those in Figure 3 shows that biodiesel, and diesel are less reactive than all the esters tested here.

Ignition experiments are conducted with $L = 12$ mm, and $Y_{F,1} = 0.4$. The temperature of the fuel stream, T_1 , for methyl butanoate, methyl crotonate, and ethyl propionate are $433 (\pm 10)$ K, $458 (\pm 10)$ K, and $458 (\pm 10)$ K, respectively. At chosen values of strain rate, the flow field is established. The temperature of air is increased until ignition takes place. The temperature of the oxidizer stream at ignition, $T_{2,1}$, is recorded as a function of the strain rate. Figure 7 compares the critical conditions of ignition for the esters. The experimental data for methyl decanoate was obtained from Ref. [11]. Figure 7 shows that ethyl propionate is easiest to ignite followed by methyl decanoate, methyl crotonate, and methyl butanoate. Comparison of Figures 4 and 7 shows that at a given value of strain rate, methyl decanoate, methyl crotonate, and methyl butanoate are more difficult to ignite in comparison to biodiesel.

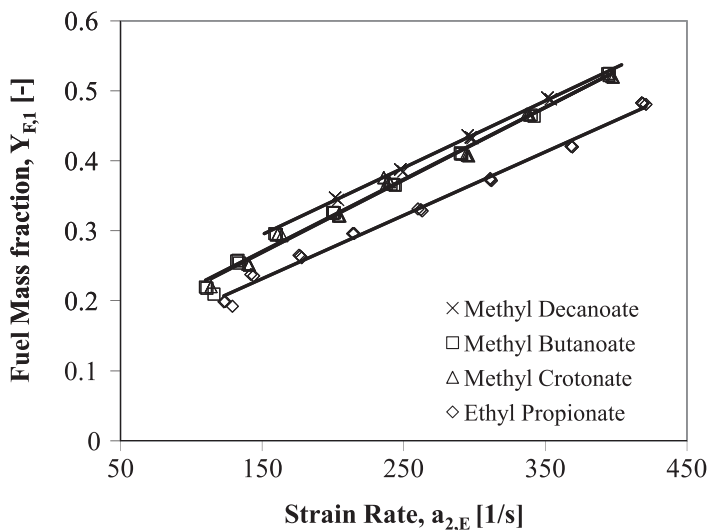


Figure 6. Experimental data showing the mass fraction of fuel in the fuel stream, $Y_{F,1}$, as a function of the strain rate, a_2 , at extinction. The symbols represent measurements. The lines are best fits to the experimental data. The experimental data was obtained employing the prevaporized fuel configuration. The experimental data for methyl decanoate was obtained from Ref. [11].

3. Kinetic modeling

Computations are performed to predict the critical conditions of extinction and ignition for methyl butanoate. A computer program called FlameMaster is used to integrate the conservation equations of mass, momentum and energy, and the species balance equations [20, 21]. The diffusion equation includes thermal diffusion, and the energy conservation

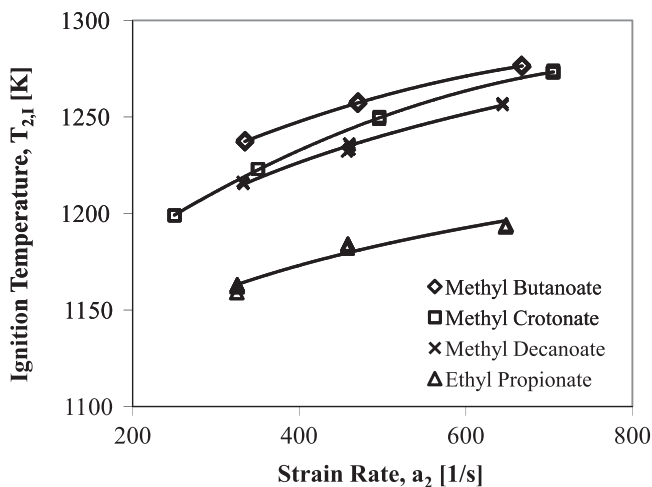


Figure 7. Experimental data showing the temperature of air at ignition, $T_{2,1}$, as a function of a_2 . The symbols represent measurements. The lines are best fits to the experimental data. The experimental data was obtained employing the prevaporized fuel configuration. The experimental data for methyl decanoate was obtained from Ref. [11].

equation includes radiative heat loss from carbon dioxide and water vapor. Buoyancy is neglected. For the axisymmetric flow considered here, there exists a similarity solution, with the radial component of flow velocity given by the product of the radial coordinate and a quantity that is a function of the axial coordinate, y [21]. The temperature and mass fraction of all species are presumed to be a function of the axial coordinate. The chemical-kinetic mechanism for methyl butanoate employed in the calculations is derived from that of Fisher et al. [6]. To facilitate the numerical computations in the quasi-one dimensional configuration, the mechanism was reduced regarding the number of reactive species. This was done by performing a number of homogeneous reactor (zero dimensional) calculations for different temperatures, pressures, and equivalence ratios. The initial temperatures chosen were 1200 K, 1600 K, and 2000 K. The pressures were 1 and 10 bar, and the equivalence ratios were 1 and 2. Over all combinations of these quantities, ignition delay times were calculated with the full mechanism, and with all mechanisms that had one species at a time removed. Based on the root-mean-square deviation from the ignition delay time of the full mechanism, the mechanism was reduced from 256 to 75 reactive species. Based on a reaction path analysis, eight more species were eliminated that were only produced but not consumed in this skeletal mechanism. The species C_2H_5OH and CH_3CHCO were eliminated since they were only formed from C_2H_5 and C_3H_6 , respectively, and did not appear to be crucial for the oxidation reactions starting with methyl butanoate. After introducing these simplifications, the chemical-kinetic employed in the numerical calculations is made up of 65 reactive species and 415 reversible reactions. This mechanism is available in Ref. [22]. It is used to calculate the critical conditions of extinction and ignition in the condensed fuel and prevaporized fuel configurations.

3.1. Condensed fuel configuration

In the condensed fuel configuration, boundary conditions are applied at the oxidizer boundary and on the gas side of the liquid–gas interface [13, 21]. At the oxidizer boundary the mass fractions of all species, except those for oxygen and nitrogen, are set equal to zero. The mass fraction of O_2 at the boundary, $Y_{O_2,2}$, is the same as in the experiments. The temperature, T_2 , at the oxidizer boundary is prescribed. The axial component of the flow velocity, V_2 , is prescribed, while the radial component of the flow velocity is set equal to zero at the oxidizer boundary. At the liquid–gas interface, mixed boundary conditions are applied for the species balance equations, and the energy conservation equation. The total mass flux of all species, i , is comprised of the diffusive flux, $j_{i,s}$, and the convective terms. This total mass flux for all species, except that for the fuel, is prescribed to vanish at the liquid–gas interface. The total mass flux of fuel evaporating from the surface of the liquid fuel is balanced by the burning rate, $\dot{m} = \rho_s V_s$. Here ρ_s is the density of the mixture on the gas side of the liquid–gas interface. The heat flux at the liquid–gas interface is balanced by the product \dot{m} and h_L . Here $h_L = 331.28$ kJ/kg is the heat of vaporization of methyl butanoate. The temperature at the liquid–gas interface is presumed to be equal to the boiling point of methyl butanoate, thus, $T_s = 375$ K. The boundary condition at the liquid–gas interface is written as [23]

$$\begin{aligned} \dot{m} Y_{i,s} + j_{i,s} &= 0, \quad i \neq F \\ \dot{m} (1 - Y_{F,s}) - j_{F,s} &= 0 \\ [\lambda (dT/dy)]_s - \dot{m} h_L &= 0 \\ T &= T_s. \end{aligned} \tag{3}$$

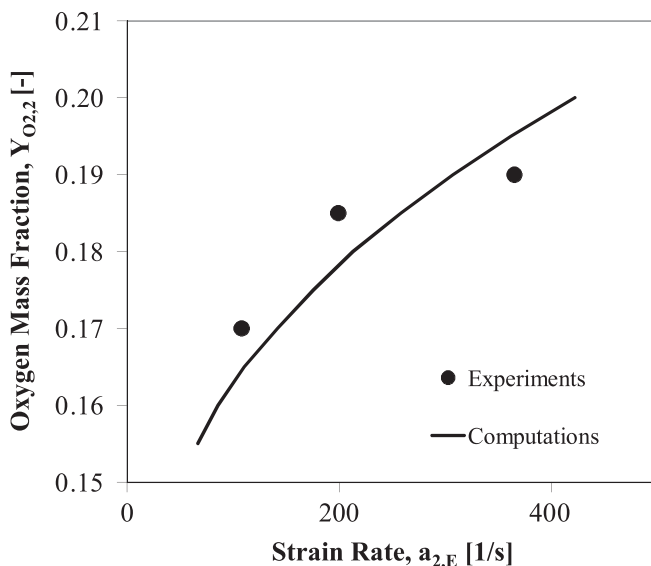


Figure 8. The mass fraction of oxygen in the oxidizer stream, $Y_{O_{2,2}}$, as a function of the strain rate, $a_{2,e}$, at extinction. The fuel is methyl butanoate. The symbols represent measurements reproduced from Figure 3. The lines are results of modeling. The experimental data and numerical calculations are obtained employing the condensed fuel configuration.

Here λ is the thermal conductivity. Heat losses from the liquid pool to the burner are neglected. It has been shown that the radial component of the flow velocity can be set equal to zero at the liquid–gas interface [13]. The mass fractions of all species at the liquid–gas interface, $Y_{i,s}$, and the burning rate, \dot{m} , are calculated.

Figures 8 and 9 compare experimental data for extinction and ignition with results obtained from modeling. These figures show that the calculated values of critical conditions of extinction and ignition agree well with experimental data. Figure 10 shows the calculated mass burning rate, \dot{m} , and the mass fraction of various species at the liquid–gas interface at conditions close to extinction. Figure 11 shows similar data at conditions close to ignition. Comparison of these figures shows that the mass fraction of fuel is high at conditions close to extinction and ignition, while the mass fraction of O_2 is very small at conditions close to extinction and high at conditions close to ignition. The values of \dot{m} at conditions close to extinction are higher than those at conditions close to ignition.

Figure 12 shows profiles of temperature and mass fractions of various species as a function of distance from the liquid–gas interface. The fuel is methyl butanoate. The profiles were calculated for flames stabilized in the condensed fuel configuration for $Y_{O_{2,2}}=0.21$, temperature $T_2=298$, and the strain rate $a_2=200\text{ s}^{-1}$. The figure shows profiles of the reactants methyl butanoate ($C_5H_{10}O_2$) and oxygen (O_2), the intermediate species carbon monoxide (CO) and hydrogen (H_2), the radical H, and the stable products carbon dioxide (CO_2) and water vapor (H_2O). The fuel boundary is at $y=0$. The gradient of temperature with respect to the axial coordinate, and the gradient of mass fraction of all species, except that of H, is not zero at the fuel boundary. The gradient and value of these quantities satisfy the boundary condition at the liquid–gas interface given by Equation (3). The asymptotic structure of the methyl butanoate flame shown in Figure 12 is similar to the asymptotic structure of many hydrocarbon and alcohol flames [24–26]. Figure 12 shows that the mass

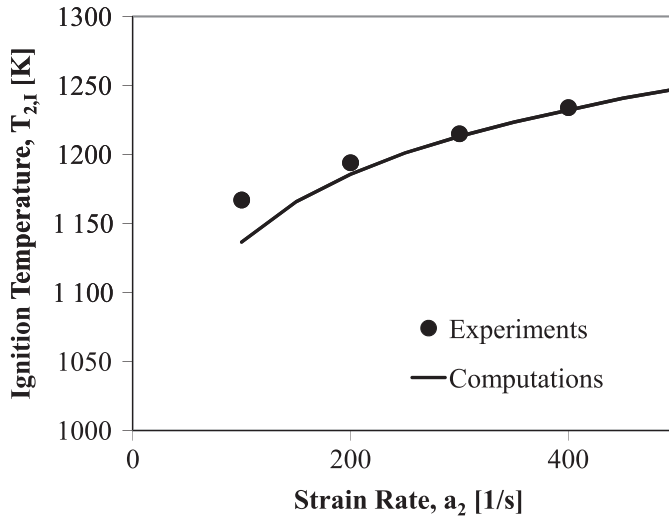


Figure 9. The temperature of air at ignition, $T_{2,1}$, as a function of the strain rate, a_2 . The fuel is methyl butanoate. The symbols represent measurements reproduced from Figure 4. The lines are results of modeling. The experimental data and numerical calculations are obtained employing the condensed fuel configuration.

fraction of methyl butanoate and H radical approach zero at about the same location, and the peak value of CO and H₂ is located close to this position. The peak value of temperature and mass fractions of CO₂ and H₂O is observed on the right side of the position where the concentration of fuel is very small and where the peak values of CO and H₂O are observed. This is consistent with the asymptotic description of the flame structure where the reaction zone is separated into two layers – an inner layer, and an oxidation

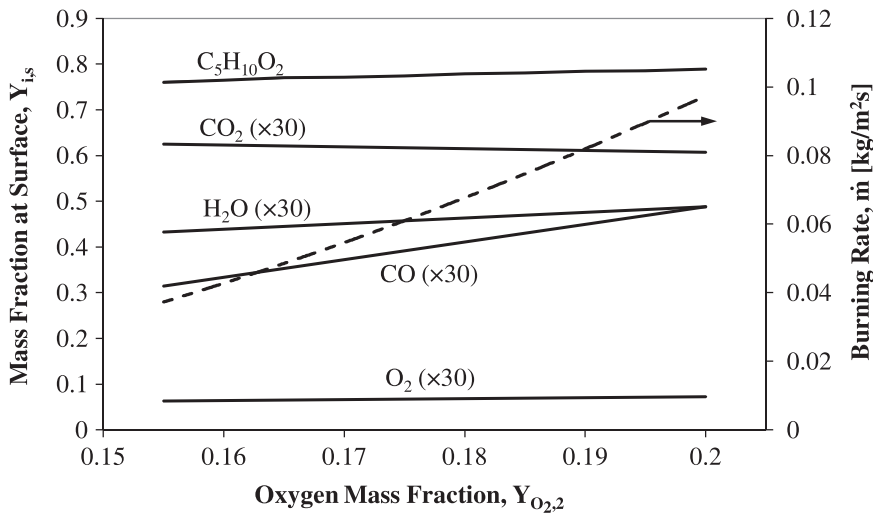


Figure 10. Calculated values the mass burning rate \dot{m} , and the mass fraction of various species at the liquid–gas interface, as a function of the mass fraction of oxygen in the oxidizer stream at conditions close to extinction.

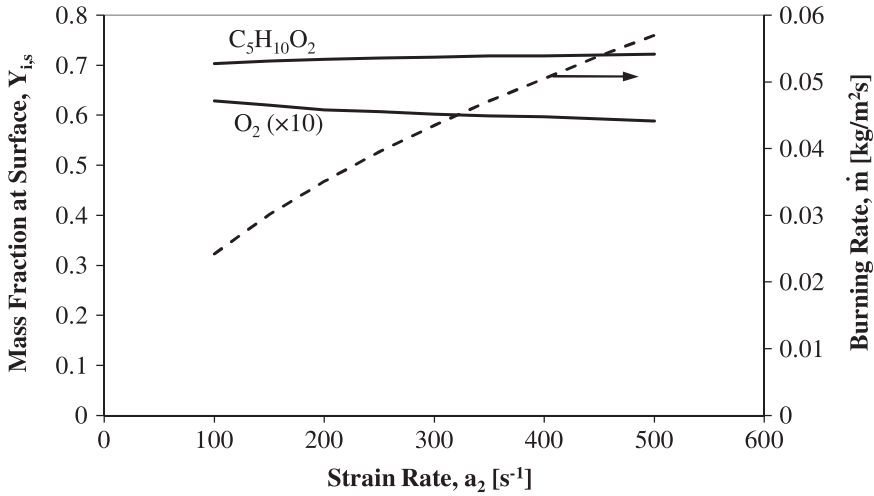


Figure 11. Calculated values the mass burning rate \dot{m} , and the mass fraction of various species at the liquid–gas interface, as a function of the strain rate at conditions close to ignition.

layer [24–26]. In the inner layer, fuel reacts with radicals and the intermediate species CO and H₂ are formed. The intermediate species are oxidized to CO₂ and H₂O in the oxidation layer.

3.2. Prevaporized fuel configuration

In this configuration, the boundary conditions at the oxidizer boundary are similar to those for the condensed fuel configuration. At the fuel boundary the mass fraction of all species

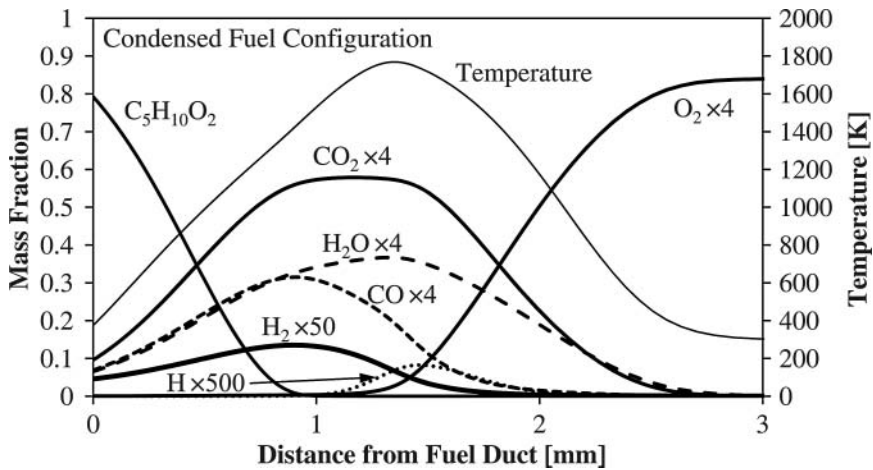


Figure 12. Profiles of temperature and mass fractions of various species as a function of distance from the liquid–gas interface. The fuel is methyl butanoate. The profiles were calculated for flames stabilized in the condensed fuel configuration for $Y_{O_2,2}=0.21$, temperature $T_2=298$, and the strain rate $a_2=200 \text{ s}^{-1}$.

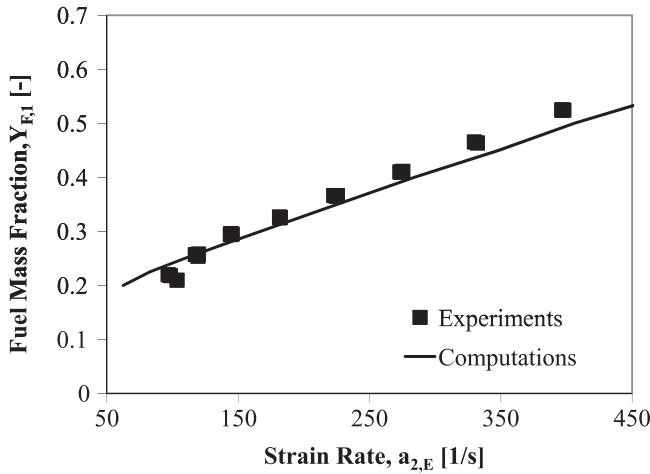


Figure 13. The mass fraction of fuel in the fuel stream, $Y_{F,1}$, as a function of the strain rate, $a_{2,e}$, at extinction. The fuel is methyl butanoate. The symbols represent measurements reproduced from Figure 6. The lines are results of modeling. The experimental data and numerical calculations are obtained employing the prevaporized fuel configuration.

except those of fuel and nitrogen are set equal to zero. The axial flow velocities, V_1 and V_2 , and the temperatures, T_1 and T_2 , are prescribed, while the radial flow velocities at the boundaries are set equal to zero. Figures 13 and 14 show that the critical conditions of extinction and ignition calculated using the kinetic model agrees well with experimental data. Thus the kinetic model accurately predicts experimental data on critical conditions of extinction and ignition obtained in the condensed fuel and prevaporized fuel configurations.

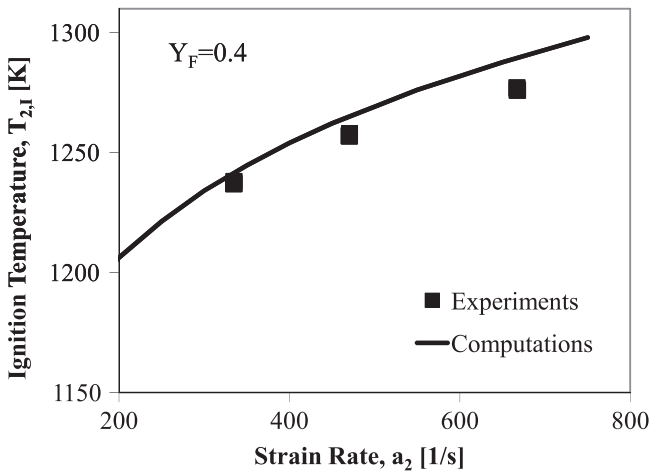


Figure 14. The temperature of air at ignition, $T_{2,1}$, as a function of the strain rate, a_2 . The fuel is methyl butanoate. The symbols represent measurements reproduced from Figure 7. The lines are results of modeling. The experimental data and numerical calculations are obtained employing the prevaporized fuel configuration.

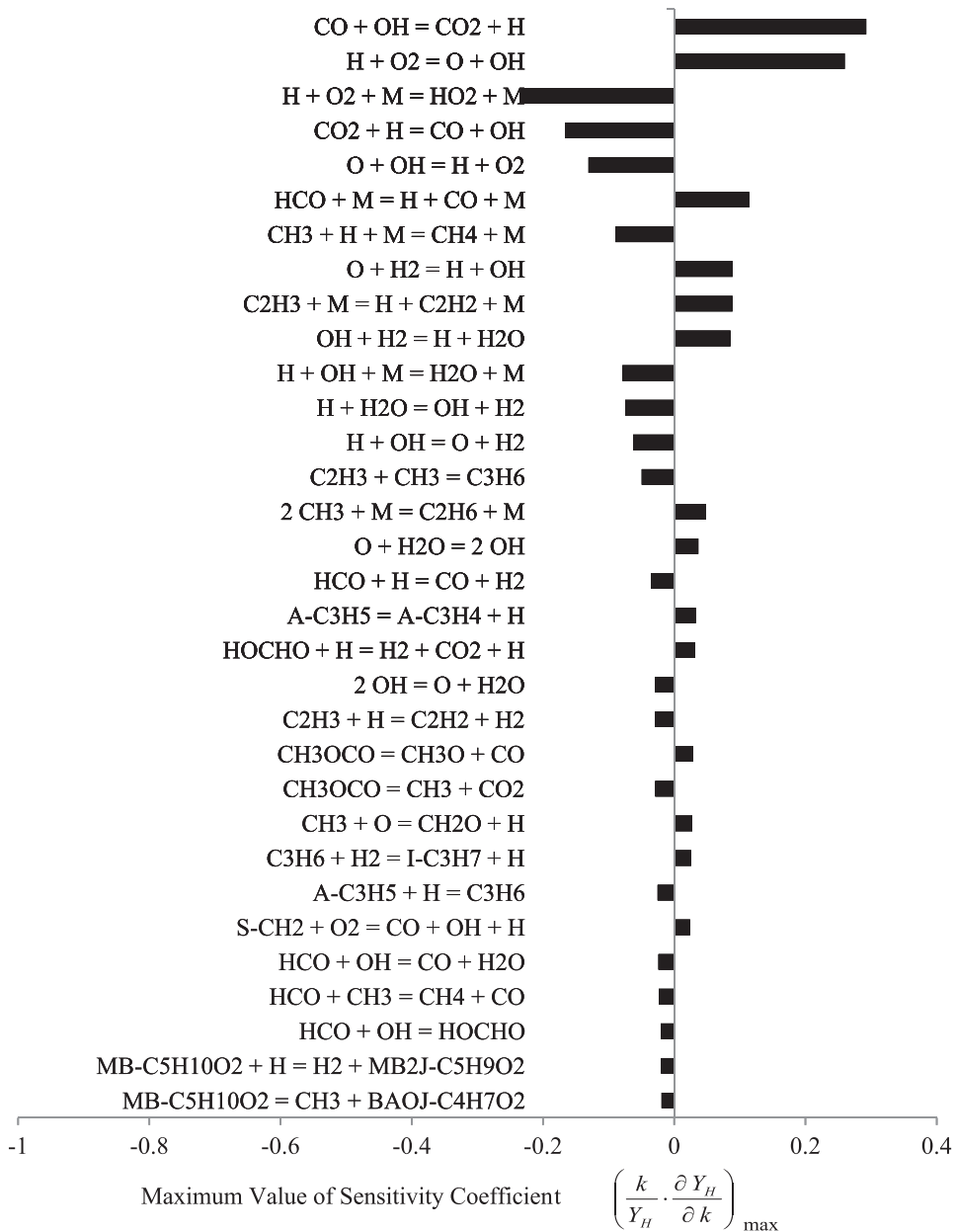


Figure 15. Sensitivity coefficient for various elementary reactions. The fuel is methyl butanoate. The sensitivity coefficients were calculated for flames stabilized in the prevaporized fuel configuration for $Y_{O_2,2}=0.233$, the temperature $T_2 = 298$, $Y_{F,1} = 0.5$, $T_1 = 453$ K and the strain rate $a_2 = 200$ s⁻¹.

This confirms the accuracy of the experimental data, the chemical-kinetic mechanism, and the kinetic modeling.

Figure 15 shows the maximum value of the sensitivity coefficient for various elementary reactions given by $[(k/Y_H)(\partial k/\partial Y_H)]_{\max}$. Here k is the rate constant and Y_H is the mass fraction of H. The fuel is methyl butanoate. The sensitivity coefficients were calculated for

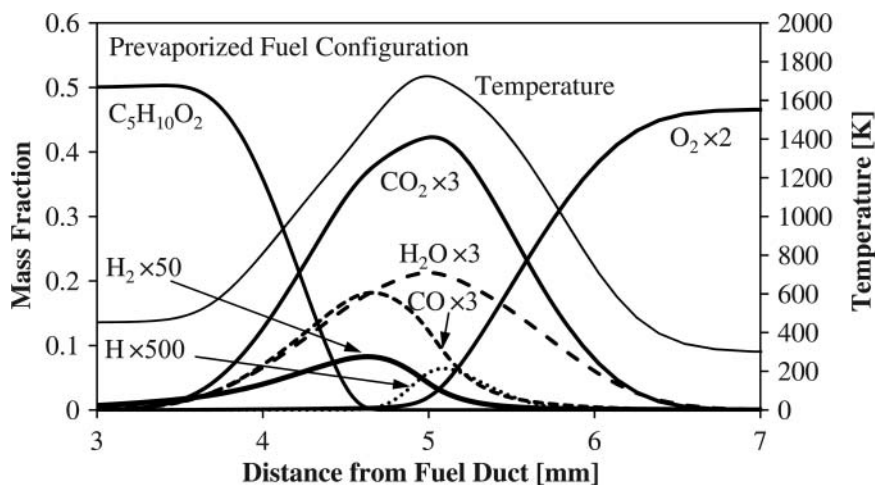


Figure 16. Profiles of temperature and mass fractions of various species as a function of distance from the fuel boundary. The fuel is methyl butanoate. The profiles were calculated for flames stabilized in the prevaporized fuel configuration for $Y_{O_2,2} = 0.233$, $T_2 = 298$, $Y_{F,1} = 0.5$, $T_1 = 453$ K, and the strain rate $a_2 = 200$ s⁻¹.

flames stabilized at $Y_{O_2,2} = 0.233$, $T_2 = 298$, $Y_{F,1} = 0.5$, $T_1 = 453$ K, and the strain rate $a_2 = 200$ s⁻¹. Previous studies have established that the radicals H and OH play key roles in extinction and ignition of flames in nonuniform flows [25–27]. These radicals participate in fuel breakdown reactions, chain branching reactions and chain breaking reactions [25,26]. Seiser et al. [27] used OH radicals in their sensitivity analysis of ignition of *n*-heptane in nonuniform flows. It is noteworthy that the first 17 reactions that are found to be important in combustion of methyl butanoate are also of importance in combustion of many hydrocarbon compounds [25,26]. The twenty-third reaction in Figure 15 is $\text{CH}_3\text{OCO} \rightleftharpoons \text{CH}_3 + \text{CO}_2$. The importance of this reaction indicates that, for the oxygenated fuel considered here, some CO_2 is also formed in the inner-layer. This explains the broad CO_2 profile observed in Figure 12 when compared with that of H_2O .

Figure 16 shows the flame structure calculated in the prevaporized configuration. The profiles were calculated at conditions similar to those in Figure 15. The asymptotic flame structure in Figure 16 is similar to that calculated for the same fuel, in the condensed fuel configuration shown in Figure 12. The key difference between the structures is that in Figure 16 the gradient of temperature with respect to the axial coordinate, and the gradient of mass fraction of all species, is zero at the fuel boundary. This is again consistent with the boundary conditions applied at the fuel boundary.

4. Concluding remarks

The condensed fuel configuration is useful for experimental studies on those liquid fuels that have high boiling points. The ignition temperature for biodiesel is very close to that for diesel. A reduced kinetic model for methyl butanoate derived from the mechanism described in Ref. [6] accurately predicts critical conditions of extinction and ignition in the condensed fuel configuration and in the prevaporized fuel configuration. This indicates that combustion of low molecular weight esters such as methyl butanoate could be described satisfactorily using available kinetic models, even when extended to reactive

flow systems. More research needs to be done to test how good surrogate fuels made up of low molecular weight hydrocarbons and esters can predict the combustion of practical fuels such as diesel and biodiesel. For example, oxygenate compounds such as alcohols or ethers have generally lower cetane numbers than the corresponding straight chain hydrocarbons, which means they are harder to ignite in diesel engines. On the other hand, in certain nonpremixed combustion configurations, the diffusion of fuel to the reaction zone can be an important factor, and here, low molecular weight hydrocarbons and esters can cause ignition temperatures to be lower. These two offsetting factors can make low molecular weight hydrocarbon fuels and esters sometimes behave similar to larger practical fuels. The validation of chemical-kinetic models for low molecular weight compounds sets the stage for extending mechanisms to larger molecular weight hydrocarbon fuels and esters, and these are expected to even better serve as surrogate fuels for diesel and biodiesel.

Acknowledgments

The authors thank Mr. Tei Newmann-Lehman for his assistance in preparing this manuscript, and the early contribution to this work by Dr. Stefan H. Humer and Mr. Justin Gerritzen. The research is supported by UC Discovery/Westbiofuels, Grant # GCP06-10228, and by the US Army Research Office, Grant # W911NF-09-1-0108.

References

- [1] C. Westbrook, W. Pitz, P. Westmoreland, F. Dryer, M. Chaos, P. Osswald, K. Kohse-Höinghaus, T. Cool, J. Wang, B. Yang, N. Hansen, and T. Kasper, *A detailed chemical kinetic reaction mechanism for oxidation of four small alkyl esters in laminar premixed flames*, Proc. Combust. Inst. 32 (2009), pp. 221–228.
- [2] M.H. Hakka, P.A. Glaude, O. Herbinet, and F. Battin-Leclerc, *Experimental study of the oxidation of large surrogates for diesel and biodiesel fuels*, Combust. Flame 156 (2009), pp. 2129–2144.
- [3] C. Hayes and D. Burgess, *Exploring the oxidative decompositions of methyl esters: Methyl butanoate and methyl pentanoate as model compounds for biodiesel*, Proc. Combust. Inst. 32 (2009), pp. 263–270.
- [4] S. Dooley, H. Curran, and J. Simmie, *Autoignition measurements and a validated kinetic model for the biodiesel surrogate, methyl butanoate*, Combust. Flame 153 (2008), pp. 2–32.
- [5] S. Gail, M. Thomson, S. Sarathy, S. Syed, P. Dagaut, P. Diévar, A. Marchese, and F. Dryer, *A wide-ranging kinetic modeling study of methyl butanoate combustion*, Proc. Combust. Inst. 31 (2007), pp. 305–311.
- [6] E.M. Fisher, W.J. Pitz, H.J. Curran, and C.K. Westbrook, *Detailed chemical kinetic mechanisms for combustion of oxygenated fuels*, Proc. Combust. Inst. 28 (2000), pp. 1579–1586.
- [7] S. Sarathy, S. Gail, S. Syed, M. Thomson, and P. Dagaut, *A comparison of saturated and unsaturated C₄ fatty acid methyl esters in an opposed flow diffusion flame and a jet stirred reactor*, Proc. Combust. Inst. 31 (2007), pp. 1015–1022.
- [8] J.P. Szybist and A.L. Boehman, *Auto-Ignition Behavior of Methyl Decanoate*, Vol. 50, American Chemical Society, 2005.
- [9] P. Dagaut, S. Gail, and M. Sahasrabudhe, *Rapeseed oil methyl ester oxidation over extended ranges of pressure, temperature, and equivalence ratio: Experimental and modeling kinetic study*, Proc. Combust. Inst. 31 (2007), pp. 2955–2961.
- [10] O. Herbinet, W.J. Pitz, and C.K. Westbrook, *Detailed chemical kinetic oxidation mechanism for a biodiesel surrogate*, Combust. Flame 154 (2008), pp. 507–528.
- [11] K. Seshadri, T. Lu, O. Herbinet, S. Humer, U. Niemann, W.J. Pitz, R. Seiser, and C.K. Law, *Experimental and kinetic modeling study of extinction and ignition of methyl decanoate in laminar non-premixed flows*, Proc. Combust. Inst. 32 (2009), pp. 1067–1074.

- [12] O. Herbinet, W.J. Pitz, and C.K. Westbrook, *Detailed chemical kinetic mechanism for the oxidation of biodiesel fuels blend surrogate*, *Combust. Flame* 157 (2010), pp. 893–908.
- [13] K. Seshadri, S. Humer, and R. Seiser, *Activation-energy asymptotic theory of autoignition of condensed hydrocarbon fuels in non-premixed flows with comparison to experiment*, *Combust. Theory Model.* 12 (2008), pp. 831–855.
- [14] A. Hamins, *The Structure and Extinction of Diffusion Flames*, University of California, San Diego, 1985.
- [15] A. Hamins and K. Seshadri, *The structure of diffusion flames burning pure, binary, and ternary solutions of methanol, heptane, and toluene*, *Combust. Flame* 68 (1987), pp. 295–307.
- [16] K. Seshadri and F.A. Williams, *Laminar flow between parallel plates with injection of a reactant at high Reynolds number*, *Int. J. Heat Mass Transf.* 21 (1978), pp. 251–253.
- [17] A. Hamins and K. Seshadri, *Structure of counterflow diffusion flames burning multicomponent fuels*, in *Twentieth Symposium (International) on Combustion* The Combustion Institute, Pittsburgh, Pennsylvania, 1984, pp. 1905–1913.
- [18] K. Seshadri, S. Humer, and R. Seiser, *Activation-energy asymptotic theory of autoignition of condensed hydrocarbon fuels in non-premixed flows with comparison to experiment*, *Combust. Theory Model.* 12 (2008), pp. 831–855.
- [19] R. Seiser, K. Seshadri, E. Piskernik, and A. Liñán, *Ignition in the viscous layer between counterflowing streams: Asymptotic theory with comparison to experiments*, *Combust. Flame* 122 (2000), pp. 339–349.
- [20] H. Pitsch, *Entwicklung eines Programmpaketes zur Berechnung eindimensionaler Flammen am Beispiel einer Gegenstromdiffusionsflamme*; Master's thesis, RWTH Aachen, Germany, 1993.
- [21] N. Peters, *Flame calculations with reduced mechanisms – an outline*, in *Reduced Kinetic Mechanisms for Applications in Combustion Systems*, N. Peters and B. Rogg, eds., *Lecture Notes in Physics*, Vol. 15, Springer Verlag, Heidelberg, 1993, chap. 1, pp. 3–7.
- [22] <http://combustion.ucsd.edu/mechanisms/methylbutanoate/ctm/>.
- [23] C.M. Müller, K. Seshadri, and J.Y. Chen, *Reduced kinetic mechanisms for counterflow methanol diffusion flames*, in *Reduced Kinetic Mechanisms for Applications in Combustion Systems*, N. Peters and B. Rogg, eds., Springer-Verlag, Berlin, 1993, chap. 16, pp. 284–307.
- [24] B. Yang and K. Seshadri, *The asymptotic structure of methanol–air diffusion flames*, *Combust. Sci. Technol.* 97 (1994), pp. 193–218.
- [25] K. Seshadri and F.A. Williams, *Reduced chemical systems and their application in turbulent combustion*, in *Turbulent Reacting Flows*, P.A. Libby and F.A. Williams, eds., Academic Press, San Diego, 1994, pp. 153–210.
- [26] K. Seshadri, *Multistep asymptotic analyses of flame structures*, *Proc. Combust. Inst.* 26 (1996), pp. 831–846.
- [27] R. Seiser, H. Pitsch, K. Seshadri, W.J. Pitz, and H.J. Curran, *Extinction and autoignition of n-heptane in counterflow configuration*, *Proc. Combust. Inst.* 28 (2000), pp. 2029–2037.